

# Denosumab Reduces Cortical Porosity of the Proximal Femoral Shaft in Postmenopausal Women With Osteoporosis

Roger Zebaze,<sup>1</sup> Cesar Libanati,<sup>2</sup> Michael R McClung,<sup>3</sup> José R Zanchetta,<sup>4</sup> David L Kendler,<sup>5</sup> Arne Høiseth,<sup>6</sup> Andrea Wang,<sup>2</sup> Ali Ghasem-Zadeh,<sup>1</sup> and Ego Seeman<sup>1</sup>

<sup>1</sup>Austin Health, University of Melbourne, Melbourne, Australia

<sup>2</sup>Amgen Inc., Thousand Oaks, CA, USA

<sup>3</sup>Oregon Osteoporosis Center, Portland, OR, USA

<sup>4</sup>Instituto de Investigaciones Metabólicas, Buenos Aires, Argentina

<sup>5</sup>University of British Columbia, Vancouver, BC, Canada

<sup>6</sup>Curato Røntgen, Oslo, Norway

## ABSTRACT

Hip fractures account for over one-half the morbidity, mortality, and cost associated with osteoporosis. Fragility of the proximal femur is the result of rapid and unbalanced bone remodeling events that excavate more bone than they deposit, producing a porous, thinned, and fragile cortex. We hypothesized that the slowing of remodeling during treatment with denosumab allows refilling of the many cavities excavated before treatment now opposed by excavation of fewer new resorption cavities. The resulting net effect is a reduction in cortical porosity and an increase in proximal femur strength. Images were acquired at baseline and 36 months using multidetector CT in 28 women receiving denosumab and 22 women receiving placebo in a substudy of FREEDOM, a randomized, double-blind, placebo-controlled trial involving women with postmenopausal osteoporosis. Porosity was quantified using StrAx1.0 software. Strength was estimated using finite element analysis. At baseline, the higher the serum resorption marker, CTx, the greater the porosity of the total cortex ( $r = 0.34$ ,  $p = 0.02$ ), and the higher the porosity, the lower the hip strength ( $r = -0.31$ ,  $p = 0.03$ ). By 36 months, denosumab treatment reduced porosity of the total cortex by 3.6% relative to baseline. Reductions in porosity relative to placebo at 36 months were 5.3% in total cortex, 7.9% in compact-appearing cortex, 5.6% in outer transitional zone, and 1.8% in inner transitional zone (all  $p < 0.01$ ). The improvement in estimated hip integral strength of 7.9% from baseline ( $p < 0.0001$ ) was associated with the reduction in total porosity ( $r = -0.41$ ,  $p = 0.03$ ). In summary, denosumab reduced cortical porosity of the proximal femoral shaft, resulting in increased mineralized matrix volume and improved strength, changes that may contribute to the reduction in hip and nonvertebral fractures reported with denosumab therapy. © 2016 The Authors. *Journal of Bone and Mineral Research* published by Wiley Periodicals, Inc. on behalf of American Society for Bone and Mineral Research (ASBMR).

**KEY WORDS:** DISEASES OF THE BONE–OSTEOPOROSIS; ANALYSIS/QUANTIFICATION OF BONE–OTHER; PRACTICE–FRACTURE PREVENTION; THERAPEUTICS–OTHER

## Introduction

Vertebral fractures have served as hallmarks of osteoporosis for over 70 years. Indeed, the reduction of vertebral fracture risk is the primary endpoint in clinical trials despite evidence that nonvertebral fractures account for over 70% of all fragility fractures.<sup>(1,2)</sup> Of these, hip fractures are responsible for significant morbidity, mortality, and cost in the community.<sup>(2,3)</sup>

The fragility of the proximal femur in advanced age is the result of two abnormalities in bone remodeling. After menopause, remodeling becomes unbalanced and rapid; more bone is resorbed than deposited by large numbers of remodeling units initiated upon the intracortical, endocortical, and trabecular surfaces.<sup>(4)</sup> Rapid remodeling upon trabecular surfaces produces trabecular bone loss, thinning, and perforation of the trabeculae.

This is an open access article under the terms of the Creative Commons Attribution-NonCommercial-NoDerivs License, which permits use and distribution in any medium, provided the original work is properly cited, the use is non-commercial and no modifications or adaptations are made.

Received in original form November 16, 2015; revised form April 6, 2016; accepted April 13, 2016. Accepted manuscript online April 15, 2016.

Address correspondence to: Ego Seeman, MD, Department of Endocrinology, Level 2, Centaur Building, Repatriation Campus, Austin Health, Waterdale Rd, Heidelberg 3081, Melbourne, Australia. E-mail: egos@unimelb.edu.au

Current address: Cesar Libanati, UCB Pharma, Brussels, Belgium.

Public clinical trial registration: <http://clinicaltrials.gov/show/NCT00089791>. A Study to Evaluate Denosumab in the Treatment of Postmenopausal Osteoporosis FREEDOM (Fracture REduction Evaluation of Denosumab in Osteoporosis Every 6 Months).

*Journal of Bone and Mineral Research*, Vol. xx, No. xx, Month 2016, pp 1–8

DOI: 10.1002/jbmr.2855

© 2016 The Authors. *Journal of Bone and Mineral Research* published by Wiley Periodicals, Inc. on behalf of American Society for Bone and Mineral Research (ASBMR)

However, most age-related bone loss is cortical in origin because approximately 80% of the skeleton is cortical.<sup>(5-7)</sup> Cortical bone is eroded by unbalanced and rapid remodeling upon the endocortical and intracortical surfaces. Of this bone loss, most is the result of intracortical remodeling initiated upon canal surfaces.<sup>(7)</sup> The canals enlarge focally and those traversing the inner cortex adjacent to the medullary canal enlarge and eventually coalesce, producing irregularly shaped large pores when viewed in cross section.<sup>(7)</sup> Porosity increases throughout the cortex and cavitation of the inner cortex 'trabecularizes' this region, forming a transitional zone between the increasingly porous and thinner but still compact-appearing subperiosteal cortex and the trabecular bone within the medullary canal.<sup>(7)</sup> The increase in porosity produces a reciprocal decrease in matrix volume and an exponential reduction in bone's ability to resist bending.<sup>(8,9)</sup>

Denosumab, a fully human RANKL monoclonal antibody, reduces the risk of vertebral, hip, and nonvertebral fractures by targeting both the imbalance in bone remodeling and the rate of remodeling.<sup>(10)</sup> Within hours of subcutaneous administration, the activity and lifespan of osteoclasts in existing remodeling units is reduced, aborting further excavation of resorption cavities, whereas the appearance of new remodeling sites is virtually abolished due to the inhibition of RANKL-mediated osteoclastogenesis.<sup>(11,12)</sup>

By inhibiting existing resorption and most subsequent remodeling during therapy, denosumab should either slow or stop any further decline in areal bone mineral density (aBMD). However, denosumab treatment increases aBMD of the axial and appendicular skeleton. Studies in nonhuman primate models suggest that the increase in aBMD is associated with a reduction in cortical porosity.<sup>(13)</sup> Studies in human subjects also demonstrate that denosumab treatment reduces porosity, but this has only been demonstrated at the distal radius.<sup>(14)</sup>

We hypothesized that the increase in proximal femoral cortical thickness, mass, aBMD, and volumetric BMD (vBMD) associated with denosumab treatment is associated with a reduction in porosity of the proximal femoral compact-appearing cortex and the transitional zone, and increases strength estimated in vivo using finite element analysis (FEA).<sup>(15-19)</sup>

## Patients and Methods

### Participants

Participants were a subset of the FREEDOM trial (ClinicalTrials.gov number, NCT00089791); the design has been reported.<sup>(10)</sup> In brief, this was an international, multicenter, randomized, double-blind, placebo-controlled study involving 7808 postmenopausal women with osteoporosis. Participants randomized to the treatment arm ( $n=3902$ ) received subcutaneous denosumab (60 mg) every 6 months. Those randomized to the placebo arm ( $n=3906$ ) received a subcutaneous placebo injection every 6 months. All subjects received daily calcium and vitamin D supplements. A subset of subjects was enrolled in a QCT imaging substudy. Calibration issues and unavailability of analyzable scans limited the analyses to 58 subjects for the hip ( $n=32$  denosumab,  $n=26$  placebo). The primary results of this substudy have been reported.<sup>(20)</sup> The analyses in this work were undertaken in the same subset of subjects with QCT scans at baseline and 36 months that were without movement artifact to allow quantification of porosity ( $n=28$  denosumab,  $n=22$  placebo). The study was conducted in accordance with all

country regulations, the Declaration of Helsinki, and the International Conference on Harmonisation Good Clinical Practice Guidelines. All subjects provided written informed consent prior to enrollment.

### Quantification of cortical porosity

Cortical porosity was measured, blinded to treatment, in five consecutive slices, 0.5 mm pixel size, and 0.7 mm slice thickness, distal to the lesser trochanter from CT scans of the proximal femur. Cortices in this region of interest (ROI) were 4 to 7 mm thick and were captured by 8 to 14 voxels, allowing delineation of cortical edges despite the 500  $\mu\text{m}$  voxel size. This is similar to HRpQCT measurements at the distal radius where cortices are 1 mm thick and the resolution is  $\sim 100 \mu\text{m}$ ; 10 voxels within the cortex.

Bone was segmented from background and into its compartments using StrAx1.0, a non-threshold-based segmentation algorithm (StraxCorp Pty Ltd, Melbourne, Australia).<sup>(21)</sup> The method automatically and reproducibly segments bone into (1) the compact-appearing cortex subjacent to periosteum, (2) the outer transitional zone adjacent to the compact-appearing cortex containing cortical fragments, (3) the inner transitional zone adjacent to the medullary canal containing cortical fragments and trabeculae abutting the cortex, and (4) trabecular bone of the medullary canal (Fig. 1). In each cortical compartment, porosity was quantified by estimating the void volume fraction of each voxel. This was achieved by quantification of the attenuation produced by background (ie, muscle) and fully mineralized bone matrix, which has a density of 1200 mg hydroxyapatite (HA)/ $\text{cm}^3$  and assigned a value of 100%. Voxels that were completely empty and had an attenuation equivalent to background were assigned a value of 0%. The volume fraction of a voxel that is void (ie, porosity) is 100% minus the mineralized bone matrix fraction.

Once deposited, osteoid is rapidly mineralized to become 'bone,' reaching  $\geq 80\%$  of full mineralization (1200 mg HA/ $\text{cm}^3$ ) within a few days. Voxels with attenuation values of  $\geq 80\%$  are unlikely to contain a pore or part of a pore, because porosity results in voxel attenuation values  $< 80\%$  of the maximum. Variations in attenuation within 80% to 100% of full mineralization are likely to reflect heterogeneity in secondary mineralization of the matrix, thus these voxels are excluded from the calculation of porosity. Voxels with attenuation  $< 80\%$  may contain a pore or part of a pore.<sup>(21)</sup>

As we have reported, StrAx1.0 facilitates quantification of porosity in low-resolution CT images even though pores are not visible to the naked eye.<sup>(22,23)</sup> The correlations between bone cross-sectional area measurement made using HRpQCT (XtremeCT; Scanco Medical AG, Brüttisellen, Switzerland) and clinical CT, of the same ROI at the subtrochanteric region of the proximal femur in 11 cadaveric specimens, ranged from  $r=0.99$  (for the entire bone and for the total cortex) to 0.95 (for the inner transitional zone) (Fig. 2A). The percentage volume occupied by pores within those bone regions was identified by StrAx1.0 regardless of the resolution of the image; the correlation between porosity measured by HRpQCT and the lower resolution CT method was 0.94 for total cortical porosity, and 0.93, 0.90, and 0.86 for porosity of the compact-appearing cortex and outer and inner transitional zones, respectively (Fig. 2B). The Bland-Altman plot showed that the error (difference between measurements by CT and HRpQCT scanning) ranged from 0% to 10% depending on the compartment, and agreement between

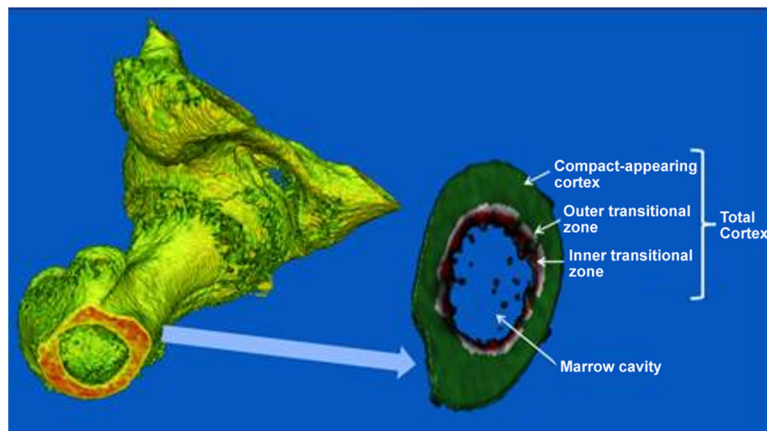


**Fig. 1.** Cross-section image of proximal femur and its compartments. Segmented computed tomography image obtained at the proximal femur using StrAx1.0, a non-threshold-based segmentation algorithm, showing the total cortex (the area used for the cortical porosity measurements), consisting of the three cortical compartments: compact-appearing cortex, outer and inner (red) transitional zones, and trabecular bone area. Porosity was assessed from QCT slices distal to the lesser trochanter.

both measurements exceeded 90% (Fig. 2C). The in vivo and ex vivo precision error was < 4%.<sup>(21–23)</sup>

#### Measurement of bone resorption, BMD, mass, thickness, and strength

Morning fasting samples were obtained at baseline in all subjects for measurement of serum CTx (sCTX), a marker of bone resorption. Serum CTx was measured with the use of ELISA (Nordic Bioscience Diagnostics A/S, Herlev, Denmark). DXA scans were analyzed to assess aBMD at the total hip.<sup>(10)</sup> QCT scans of the hip were performed at 120 kV, a pitch of 1, using 170 mA, reconstructed using a 400 mm field of view, a slice thickness of  $\leq 1.25$  mm, and a medium kernel at baseline.<sup>(20)</sup> Scans were analyzed in a blinded-to-treatment manner by a central laboratory (Synarc Inc., Newark, CA, USA). These scans were analyzed using Medical Image Analysis Framework (MIAF) software to assess vBMD of the total hip and compartments.<sup>(15)</sup>

Additionally, cortical 3D bone thickness maps of the hip were created from QCT scans, and cortical mass surface density maps were created.<sup>(18)</sup> To estimate strength, the QCT images were calibrated, segmented, and converted into finite element models (~40,000 elements per model), using cube-shaped, eight-noded brick elements (1.5 mm sided). Femoral strength for a simulated sideways fall was estimated blinded to treatment.<sup>(24)</sup> We report vBMD of the cortical compartment, cortical mass surface density and thickness, and strength assessed by FEA for subjects included in the porosity analysis.

#### Statistical analyses

Quantification of the percentage volume of the cortex of the proximal femur measured immediately below the lesser trochanter occupied by pores by the StrAx1.0 software included all subjects with evaluable data at baseline and 36 months. Pearson correlation coefficients were calculated to assess the

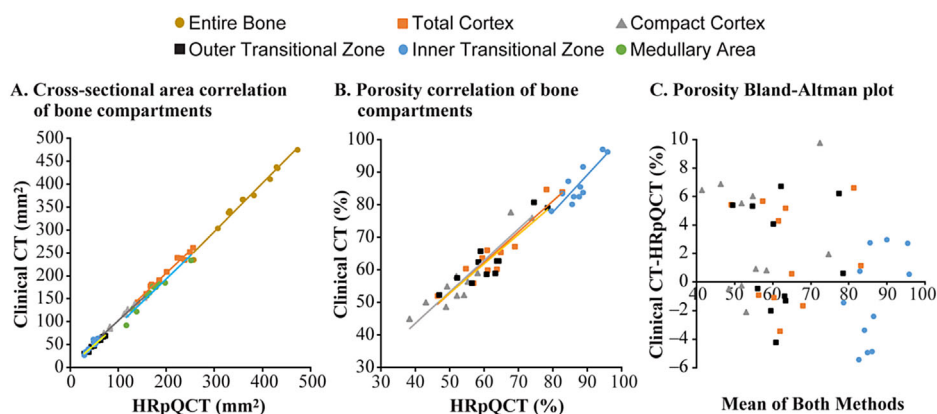


**Fig. 2.** Correlation between (A) cross-sectional areas of the cortical bone measured by HRpQCT and clinical CT, (B) porosities measured by HRpQCT and clinical CT, and (C) a Bland–Altman plot comparing porosities measured by HRpQCT and clinical CT. There were strong correlations between measurement techniques ( $r \geq 0.86$  for all bone compartments) and the Bland–Altman plot showed that the difference between measurements by CT and HRpQCT ranged from 0% to 10% depending on the compartment, and thus the agreement between both measurements exceeded 90%. Each point represents one anatomic specimen.

association between porosity and other bone measurements at baseline and change in total porosity and strength at 36 months. Baseline and 36 months porosity results were reported as mean  $\pm$  SD. Least-squares mean with two-sided 95% CI and *p* values were obtained using an ANCOVA model, adjusting for treatment and baseline value to estimate absolute or percentage change in cortical porosity, aBMD, vBMD, thickness, mass, and strength from baseline to 36 months within treatment group and the difference between groups at 36 months.

## Results

### Baseline measurements

Patient demographics, sCTx, and bone traits were comparable in the two groups at baseline (Table 1). Women with higher sCTx had higher total cortex porosity ( $r = 0.34, p = 0.02$ ). Women with higher total cortex porosity had lower aBMD ( $r = -0.37, p < 0.01$ ), lower total cortical vBMD ( $r = -0.46, p < 0.01$ ), thinner cortices ( $r = -0.33, p = 0.02$ ), lower cortical mass ( $r = -0.39, p < 0.01$ ), and lower estimated integral strength ( $r = -0.31, p = 0.03$ ) (Fig. 3A–F).

### Changes during follow-up

In the denosumab group, porosity of all cortical regions decreased relative to baseline (Table 2). The percentage change from baseline at 36 months was  $-3.6\%$  (95% CI,  $-5.2\%$  to  $-1.9\%$ )

**Table 1.** Baseline Characteristics

	Placebo ( <i>n</i> = 22) <sup>a</sup>	Denosumab ( <i>n</i> = 28) <sup>a</sup>
Age (years)	73.8 $\pm$ 6.3	73.0 $\pm$ 4.7
Body mass index (kg/m <sup>2</sup> )	24.9 $\pm$ 4.2	26.5 $\pm$ 5.3
Total hip		
T-score	$-2.0 \pm 0.7$	$-1.6 \pm 0.9$
DXA aBMD (g/cm <sup>2</sup> )	$0.7 \pm 0.1$	$0.7 \pm 0.1$
MIAF cortical vBMD (mg/cm <sup>3</sup> )	$514 \pm 54$	$533 \pm 58$
Proximal femur cortical mass	$141 \pm 18$	$145 \pm 19$
surface density (mg/cm <sup>2</sup> ) <sup>b</sup>		
Proximal femur cortical thickness	$1.2 \pm 0.2$	$1.3 \pm 0.2$
(mm) <sup>b</sup>		
Cortical volume occupied by pores (%) <sup>c</sup>		
Total	$39.5 \pm 7.6$	$40.9 \pm 11.1$
Compact-appearing cortex	$28.4 \pm 6.8$	$28.7 \pm 11.1$
Outer transitional zone	$37.5 \pm 5.4$	$36.7 \pm 8.8$
Inner transitional zone	$71.4 \pm 3.8$	$72.0 \pm 3.6$
FEA hip integral strength (N)	$2228 \pm 592$	$2460 \pm 640$
sCTx (ng/mL), median (IQR)	0.44 (0.37–0.58)	0.47 (0.34–0.69)

Data are mean  $\pm$  SD unless otherwise indicated. *n* = number of subjects with available hip porosity data at baseline and 36 months.

aBMD = areal BMD; MIAF = Medical Image Analysis Framework; vBMD = volumetric BMD; FEA = finite element analysis; sCTx = serum CTx; IQR = interquartile range; N = Newtons.

<sup>a</sup>Between-group *t* test, *p* > 0.05 for all characteristics.

<sup>b</sup>*n* = 21, placebo.

<sup>c</sup>Cortical volume is the volume enveloped by the periosteal and endocortical surface. Of this volume, 30% to 40% is void volume formed by canals traversing the cortex. In cross sections of cortex, these canals form most of the “porosity.” Porosity was assessed below the lesser trochanter.

for the total cortex,  $-6.7\%$  (95% CI,  $-9.7\%$  to  $-3.7\%$ ) for the compact-appearing cortex,  $-5.9\%$  (95% CI,  $-8.0\%$  to  $-3.8\%$ ) for the outer transitional zone, and  $-1.1\%$  (95% CI,  $-1.7\%$  to  $-0.5\%$ ) for the inner transitional zone (all *p* < 0.01) (Fig. 4). In the placebo group, porosity remained unchanged relative to baseline, with percentage differences at 36 months being  $1.7\%$  (95% CI,  $-0.1\%$  to  $3.6\%$ ),  $1.2\%$  (95% CI,  $-2.2\%$  to  $4.6\%$ ),  $-0.3\%$  (95% CI,  $-2.7\%$  to  $2.0\%$ ), and  $0.6\%$  (95% CI,  $0.0\%$  to  $1.3\%$ ) at the respective regions (Fig. 4).

At 36 months, significant differences in the denosumab group relative to placebo were observed for porosity in all cortical regions (all *p* < 0.001) (Table 2), as well as the total hip aBMD ( $5.1\%$  versus  $-0.7\%$ ), total cortical vBMD ( $5.2\%$  versus  $0.5\%$ ), cortical thickness ( $2.1\%$  versus  $-1.3\%$ ), cortical mass ( $4.2\%$  versus  $-0.9\%$ ), and FEA integral strength ( $7.9\%$  versus  $-5.0\%$ ) (all *p* < 0.0001).

In the denosumab group, the reduction in porosity was associated with an increase in estimated integral strength for total cortex ( $r = -0.41, p = 0.03$ ) (Fig. 5), compact-appearing cortex ( $r = -0.42, p = 0.02$ ), and outer transitional zone ( $r = -0.52, p < 0.01$ ).

## Discussion

We report that, prior to treatment, higher sCTx was associated with higher cortical porosity in the proximal femoral shaft, and that higher porosity was associated with lower estimated bone strength. Denosumab treatment reduced porosity of the total cortex, its compact-appearing region, and outer transitional zone. The reduction in porosity correlated with an increase in estimated strength.

Antiresorptive drugs reduce the volume of bone resorbed by osteoclasts of each remodeling unit so that the resorptive cavities become smaller.<sup>(25)</sup> However, the main mechanism responsible for a reduction in the rate of bone loss and slowing of structural deterioration is the reduction in rate of remodeling.<sup>(26,27)</sup> Previous studies have reported that denosumab treatment increased aBMD, vBMD, cortical thickness, mass, and estimated bone strength relative to previous treatment as well as controls.<sup>(15,18,24)</sup> Our findings confirm these observations and show that denosumab treatment reduces porosity at the proximal femoral shaft, as it does at the distal radius,<sup>(14)</sup> in postmenopausal women.

Several mechanisms are likely to account for the reduction in porosity, the increase in cortical thickness, mass, aBMD, and vBMD associated with denosumab treatment. Prior to treatment, remodeling is rapid. For each of the many remodeling or basic multicellular units (BMUs), the refilling phase of remodeling is delayed by about a week by a reversal or resting phase and then refilling proceeds slowly for about 3 months.<sup>(27–29)</sup>

When denosumab treatment is initiated, BMUs excavating cavities prior to treatment stop resorbing, are aborted, or enter their reversal and then refilling phase. Concurrently, denosumab rapidly abolishes the birth of new resorption sites, so that the result of refilling of many cavities excavated before treatment plus the birth of very few new cavities is a net decrease in porosity. Refilling or partial refilling of cavities excavated upon the Haversian canals and the endocortical surface increases mineralized matrix cortical volume and partly restores cortical thickness focally, so that there is a net increase in the volume of mineralized matrix enveloped by the periosteal and endocortical surfaces and a reciprocal decrease in the void volume. Secondary mineralization of matrix deposited in cavities

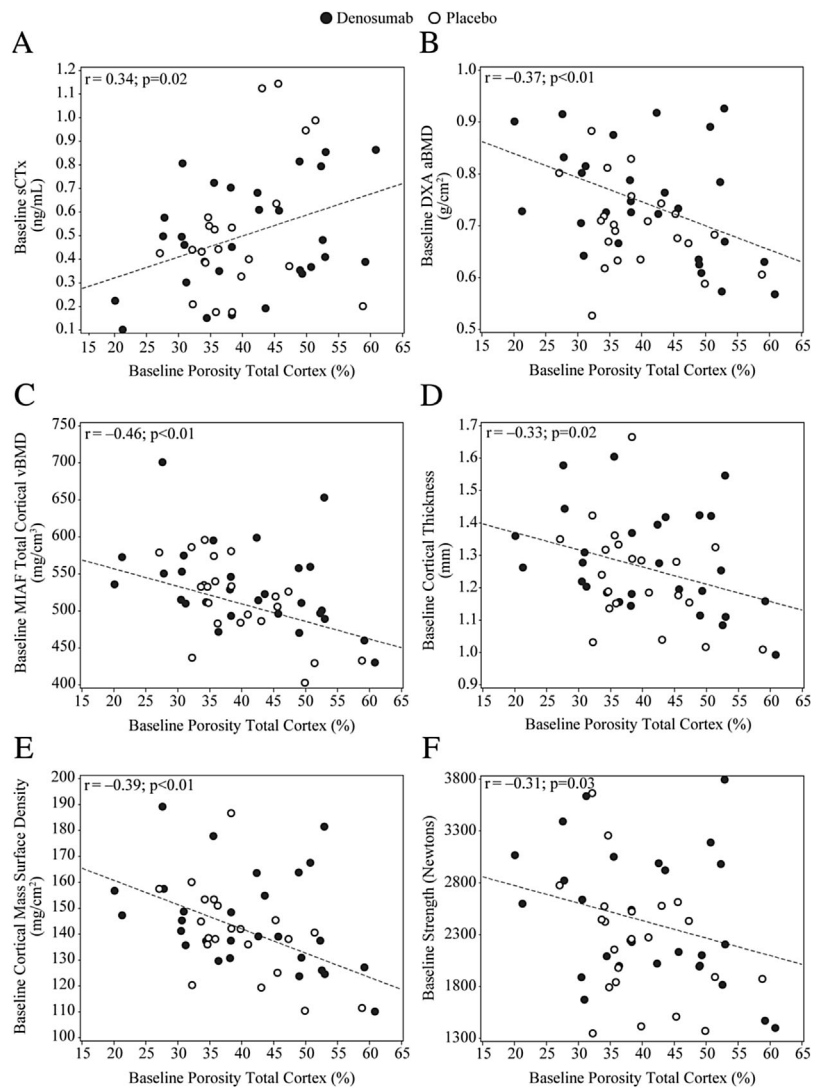


**Fig. 3.** Association between baseline proximal femoral total cortical porosity assessed distal to the lesser trochanter and (A) sCTX, (B) aBMD, (C) vBMD, (D) cortical thickness, (E) cortical mass surface density, and (F) strength. At baseline, (A) women with higher sCTX had higher total cortex porosity; (B) women with higher total cortex porosity had lower aBMD, (C) lower total cortical vBMD, (D) thinner cortices, (E) lower cortical mass, and (F) lower estimated integral strength. Regression line is based on both treatment groups combined. aBMD = areal BMD; MIAF = Medical Image Analysis Framework; sCTX = serum CTx; vBMD = volumetric BMD.

excavated prior to treatment and matrix no longer resorbed (because remodeling is suppressed) further contributes to increases in cortical vBMD.<sup>(18)</sup>

After about 12 months, a new steady state is established with remodeling proceeding slowly provided denosumab administration continues. BMD continues to increase, but more slowly for two reasons. First, secondary mineralization of recently formed osteons and osteons formed months to years earlier continues, because it can take several years to reach completion.<sup>(30)</sup> Second, studies in cynomolgus monkeys treated with denosumab suggest that, in the face of markedly reduced remodeling, modeling-based bone formation no longer obscured by high remodeling may proceed upon quiescent intracortical and endocortical surface of loaded cortical regions of the proximal femur.<sup>(13,31)</sup> This bone formation is independent of bone resorption and is unlikely to be a direct effect of

denosumab. We propose that prior to treatment, high remodeling obscures, or may remove, bone deposited by continued modeling-based bone formation throughout life. When no longer opposed by remodeling, such as achieved by denosumab administration, continued modeling could result in a prolonged net gain in bone matrix volume. This partial restoration of microstructure and increase in matrix mass may further increase bone strength and contribute to reductions in fracture rate.

This study is one of the first to report of noninvasive *in vivo* human quantification of porosity at the proximal femur, assessed at the shaft immediately distal to the lesser trochanter, using a clinically available CT technology. Although reductions in porosity of the distal radius and tibia in response to antiresorptive therapy have been reported,<sup>(14,32)</sup> these are based on the use of HRpQCT, a technique available in only a few

**Table 2.** Proximal Femoral Porosity (%) Assessed Distal to the Lesser Trochanter at Baseline, 36 Months, Absolute Change From Baseline by Treatment Group

	Placebo (n = 22)				Denosumab (n = 28)				Denosumab versus placebo
	Baseline	36 Months	Absolute change from baseline	p <sup>a</sup>	Baseline	36 Months	Absolute change from baseline	p <sup>a</sup>	
Total cortex	39.5 ± 7.6	40.1 ± 7.4	0.6	0.08	40.9 ± 11.1	39.5 ± 11.1	-1.4	<0.0001	<0.0001
Compact-appearing cortex	28.4 ± 6.8	28.7 ± 6.9	0.3	0.46	28.7 ± 11.1	27.0 ± 11.2	-1.7	<0.0001	0.0007
Outer transitional zone	37.5 ± 5.4	37.4 ± 5.7	-0.1	0.80	36.7 ± 8.8	34.7 ± 9.3	-2.0	<0.0001	0.0009
Inner transitional zone	71.3 ± 3.8	71.8 ± 3.5	0.4	0.06	72.0 ± 3.6	71.2 ± 3.7	-0.8	0.0002	0.0002

Data are mean ± SD for baseline and 36 months; absolute change from baseline data are least-squares means based on ANCOVA model adjusting for treatment and baseline value.

<sup>a</sup>p value for 36 months versus baseline within each treatment group.

<sup>b</sup>p value for denosumab versus placebo at 36 months (denosumab - placebo).

specialized centers worldwide. Additionally, these sites of fragility fracture are of less relevance in terms of morbidity and mortality than the proximal femur.

This study has several limitations. The small sample size precludes a robust assessment of the association between the changes in porosity, bone strength, or fracture. Because measurements of porosity were made at the shaft below the lesser trochanter, inferences concerning associations between changes in porosity at other regions, such as at the femoral neck, require further study. The study also cannot address to what extent the fracture risk reduction documented in FREEDOM is related to the reduction in porosity. Nevertheless, the reduction in porosity correlated with the improvement in estimated bone strength in this subset of individuals and, despite the low numbers of subjects studied, significant relations were

documented. Larger sample sizes are needed to confirm these associations. The StrAx technique is very sensitive to image quality, thus image quality without motion is essential for accurate quantification of porosity. In addition, we assumed, consistent with previous research,<sup>(21)</sup> that the area occupied only by mineralized matrix free of pores has a matrix mineral density of ≥ 80% of the maximum mineral density achievable. We cannot exclude the possibility of a small pore contributing and introducing a small error.<sup>(33)</sup> Finally, because muscle is used for calibration, fatty infiltration may introduce small errors in the results.

Image resolution of the techniques used in this study and differences in secondary mineralization may influence quantification of porosity. However, this was minimized by excluding voxels with attenuation between 80% and 100% of the

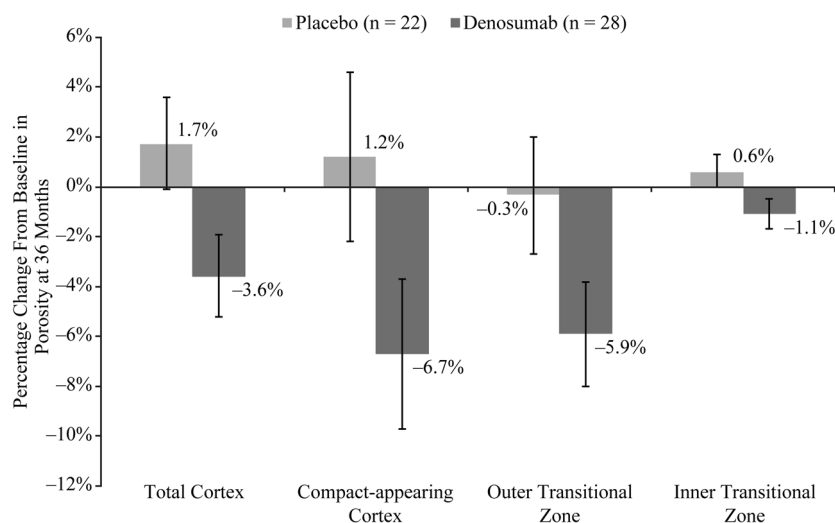


**Fig. 4.** Percentage change from baseline at 36 months in proximal femoral total cortical porosity assessed distal to the lesser trochanter in response to denosumab or placebo treatment. In the denosumab group, porosity decreased in all regions relative to baseline at 36 months. The reduction in porosity of the total cortex was mainly attributable to decreases in porosity of the compact-appearing cortex and outer transitional zone. Porosity remained unchanged relative to baseline in the placebo group. The differences in porosity in the denosumab group relative to placebo at 36 months were significant in all regions (all  $p < 0.01$ ).  $n$  = number of subjects with available data at baseline and 36 months. Data are least-squares means and 95% CIs.

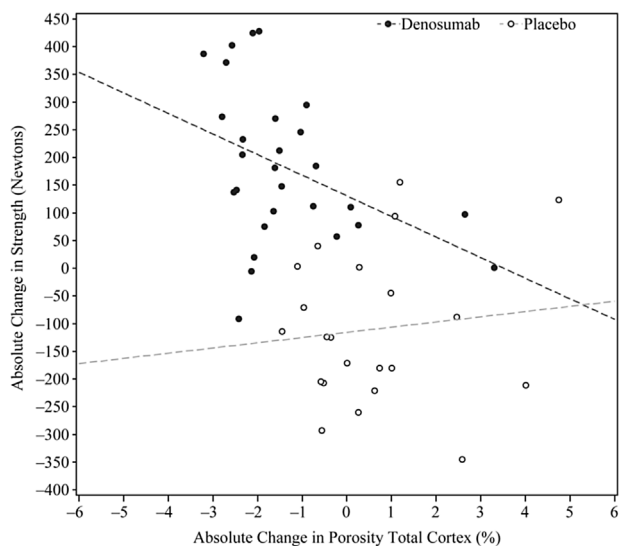


**Fig. 5.** Relationship between absolute changes in proximal femoral total cortical porosity assessed distal to the lesser trochanter and absolute changes in strength from baseline to 36 months. In the denosumab group, the reduction in porosity was associated with an increase in estimated integral strength.

maximum mineralization produced by 1200 mg HA/cm<sup>3</sup> because differences in attenuation by these voxels were most likely to be due to differences in mineralization, not porosity. Porosity, if present, would reduce attenuation below 80% of the maximum.<sup>(21)</sup> Despite the image resolution utilized, this analysis confirmed earlier work reporting that denosumab treatment reduced porosity of the cortex of the distal radius and distal tibia of postmenopausal women quantified using higher-resolution HRpQCT images, and reduced porosity of the cortex of the iliac crest of cynomolgus monkeys using histomorphometry.<sup>(13,14)</sup> Nevertheless, these changes still may be underestimated because smaller pores may not be identified at a voxel size ranging from 500 to 700  $\mu\text{m}$ .

In summary, we confirm and extend reports of *ex vivo* studies in animal models, and reports in human subjects documenting a reduction of cortical porosity associated with denosumab therapy. Quantification of cortical porosity of the hip provides a means of assessing fracture risk and the effects of treatment on this important determinant of bone strength. The benefits of denosumab treatment in reducing porosity at this location are relevant to our understanding of the structural basis of the reduced nonvertebral and hip fracture risk observed in clinical trials.

## Disclosures

RZ has received grant and/or research support from Amgen, Merck Sharp & Dohme, Servier, Warner-Chilcott, AKP, Genzyme, Sanofi, GSK, and Pfizer; he is a shareholder in StraxCorp, is remunerated by StraxCorp as president of R&D, and is one of the inventors of the StrAx1.0 algorithm; he is also a director on the board of StraxCorp. CL was an Amgen employee and may own Amgen stock and/or stock options; he is an employee and stockholder in UCB Pharma. MRM has received research grants,

consulting fees, and/or honoraria from Amgen and Merck. JRZ has received research grants and/or consulting fees from Amgen, Eli Lilly, GlaxoSmithKline, Merck Sharp & Dohme, and Radius. DLK has received research grants, consulting fees, and/or honoraria from Amgen, Astellas, AstraZeneca, Lilly, GlaxoSmithKline, Merck, and Pfizer. AH has no disclosures. AW is an Amgen employee and may own Amgen stock and/or stock options. AGZ has ownership in StraxCorp. ES has received research support from Amgen, Asahi, Genzyme, and Warner-Chilcott; he has lectured at national and international meeting symposia funded by Amgen, Merck Sharp & Dohme, Asahi, and Allergan, and has received speaker fees from Amgen, Allergan, Asahi, Merck Sharp & Dohme, and Sanofi; he is a director of the board and shareholder in StraxCorp, is remunerated by StraxCorp as chief medical officer, and is one of the inventors of the StrAx1.0 algorithm.

## Acknowledgments

This work was supported by Amgen Inc. Mandy Suggitt of Amgen Inc. assisted with the preparation of the manuscript.

Authors' roles: ES and CL were responsible for drafting the manuscript. All authors critically reviewed and revised the manuscript content and approved the final version. CL and AW take responsibility for the integrity of the data analysis.

## References

- Burge R, Dawson-Hughes B, Solomon DH, Wong JB, King A, Tosteson A. Incidence and economic burden of osteoporosis-related fractures in the United States, 2005-2025. *J Bone Miner Res.* 2007; 22(3):465-75.
- Johnell O, Kanis JA. An estimate of the worldwide prevalence and disability associated with osteoporotic fractures. *Osteoporos Int.* 2006;17(12):1726-33.
- Office of the Surgeon General (US). Bone health and osteoporosis: a report of the Surgeon General. Rockville, MD: Office of the Surgeon General; 2004.
- Seeman E, Delmas PD. Bone quality—the material and structural basis of bone strength and fragility. *N Engl J Med.* 2006;354(21): 2250-61.
- Høiseth A, Alho A, Husby T. Femoral cortical/cancellous bone related to age. *Acta Radiol.* 1990;31(6):626-7.
- Riggs BL, Wahner HW, Dunn WL, Mazess RB, Offord KP, Melton LJ 3rd. Differential changes in bone mineral density of the appendicular and axial skeleton with aging: relationship to spinal osteoporosis. *J Clin Invest.* 1981;67(2):328-35.
- Zebaze RM, Ghasem-Zadeh A, Bohte A, et al. Intracortical remodelling and porosity in the distal radius and post-mortem femurs of women: a cross-sectional study. *Lancet.* 2010;375(9727): 1729-36.
- Schaffler MB, Burr DB. Stiffness of compact bone: effects of porosity and density. *J Biomech.* 1988;21(1):13-6.
- Seeman E. Structural basis of growth-related gain and age-related loss of bone strength. *Rheumatology (Oxford).* 2008;47 Suppl 4: iv2-8.
- Cummings SR, San Martin J, McClung MR, et al. Denosumab for prevention of fractures in postmenopausal women with osteoporosis. *N Engl J Med.* 2009;361(8):756-65.
- Kostenuik PJ, Nguyen HQ, McCabe J, et al. Denosumab, a fully human monoclonal antibody to RANKL, inhibits bone resorption and increases BMD in knock-in mice that express chimeric (murine/human) RANKL. *J Bone Miner Res.* 2009;24(2):182-95.
- Lacey DL, Boyle WJ, Simonet WS, et al. Bench to bedside: elucidation of the OPG-RANK-RANKL pathway and the development of denosumab. *Nat Rev Drug Discov.* 2012;11(5):401-19.

13. Kostenuik PJ, Smith SY, Jolette J, Schroeder J, Pyrah I, Ominsky MS. Decreased bone remodeling and porosity are associated with improved bone strength in ovariectomized cynomolgus monkeys treated with denosumab, a fully human RANKL antibody. *Bone*. 2011;49(2):151–61.
14. Zebaze RM, Libanati C, Austin M, et al. Differing effects of denosumab and alendronate on cortical and trabecular bone. *Bone*. 2014;59:173–9.
15. Genant HK, Libanati C, Engelke K, et al. Improvements in hip trabecular, subcortical, and cortical density and mass in postmenopausal women with osteoporosis treated with denosumab. *Bone*. 2013;56(2):482–8.
16. Keaveny TM, Hoffmann PF, Singh M, et al. Femoral bone strength and its relation to cortical and trabecular changes after treatment with PTH, alendronate, and their combination as assessed by finite element analysis of quantitative CT scans. *J Bone Miner Res*. 2008;23(12):1974–82.
17. Keaveny TM, Kopperdahl DL, Melton LJ 3rd, et al. Age-dependence of femoral strength in white women and men. *J Bone Miner Res*. 2010;25(5):994–1001.
18. Poole KE, Treece GM, Gee AH, et al. Denosumab rapidly increases cortical bone in key locations of the femur: a 3D bone mapping study in women with osteoporosis. *J Bone Miner Res*. 2015;30(1):46–54.
19. Zysset PK, Dall'ara E, Varga P, Pahr DH. Finite element analysis for prediction of bone strength. *Bonekey Rep*. 2013;2:386.
20. McClung MR, Zanchetta JR, Høiseth A, et al. Denosumab densitometric changes assessed by quantitative computed tomography at the spine and hip in postmenopausal women with osteoporosis. *J Clin Densitom*. 2013;16(2):250–6.
21. Zebaze R, Ghasem-Zadeh A, Mbala A, Seeman E. A new method of segmentation of compact-appearing, transitional and trabecular compartments and quantification of cortical porosity from high resolution peripheral quantitative computed tomographic images. *Bone*. 2013;54(1):8–20.
22. Ahmed LA, Shigdel R, Joakimsen RM, et al. Measurement of cortical porosity of the proximal femur improves identification of women with nonvertebral fragility fractures. *Osteoporos Int*. 2015;26(8):2137–46.
23. Shigdel R, Osima M, Ahmed LA, et al. Bone turnover markers are associated with higher cortical porosity, thinner cortices, and larger size of the proximal femur and non-vertebral fractures. *Bone*. 2015;81:1–6.
24. Keaveny TM, McClung MR, Genant HK, et al. Femoral and vertebral strength improvements in postmenopausal women with osteoporosis treated with denosumab. *J Bone Miner Res*. 2014;29(1):158–65.
25. Matheny JB, Slyfield CR, Tkachenko EV, et al. Anti-resorptive agents reduce the size of resorption cavities: a three-dimensional dynamic bone histomorphometry study. *Bone*. 2013;57(1):277–83.
26. Hattner R, Epker BN, Frost HM. Suggested sequential mode of control of changes in cell behaviour in adult bone remodelling. *Nature*. 1965;206(983):489–90.
27. Parfitt AM. Skeletal heterogeneity and the purposes of bone remodelling: implications for the understanding of osteoporosis. In: Marcus R, Feldman D, Kelsey J, editors. *Osteoporosis*. San Diego, CA: Academic Press; 1996. p. 315–39.
28. Baron R. Importance of the intermediate phase between resorption and formation in the understanding and measurement of the bone remodeling sequence. In: Meunier PJ, editor. *Bone histomorphometry*. Paris: Laboratory Armour-Montagu; 1977. p. 179–83.
29. Frost HM. The skeletal intermediary organization: a synthesis. In: Pack WA, editor. *Bone and mineral research 3*. Amsterdam: Elsevier; 1985. p. 49–107.
30. Akkus O, Polyakova-Akkus A, Adar F, Schaffler MB. Aging of microstructural compartments in human compact bone. *J Bone Miner Res*. 2003;18(6):1012–9.
31. Ominsky MS, Stouch B, Schroeder J, et al. Denosumab, a fully human RANKL antibody, reduced bone turnover markers and increased trabecular and cortical bone mass, density, and strength in ovariectomized cynomolgus monkeys. *Bone*. 2011;49(2):162–73.
32. Burghardt AJ, Kazakia GJ, Sode M, de Papp AE, Link TM, Majumdar S. A longitudinal HR-pQCT study of alendronate treatment in postmenopausal women with low bone density: relations among density, cortical and trabecular microarchitecture, biomechanics, and bone turnover. *J Bone Miner Res*. 2010;25(12):2558–71.
33. Ruffoni D, Fratzi P, Roschger P, Klaushofer K, Weinkamer R. The bone mineralization density distribution as a fingerprint of the mineralization process. *Bone*. 2007;40(5):1308–19.